

## Strong Aggregation and Directional Assembly of Aromatic Oligoamide Macrocycles

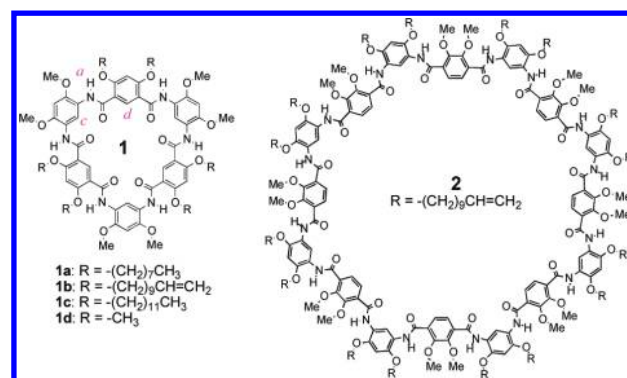
Yongan Yang,<sup>†</sup> Wen Feng,<sup>†</sup> Jinchuan Hu,<sup>†</sup> Shuliang Zou,<sup>†</sup> Rongzhao Gao,<sup>†</sup> Kazuhiro Yamato,<sup>‡</sup> Mark Kline,<sup>‡</sup> Zhonghou Cai,<sup>§</sup> Yi Gao,<sup>¶</sup> Yibing Wang,<sup>||</sup> Yibao Li,<sup>||,▽</sup> Yanlian Yang,<sup>||</sup> Lihua Yuan,<sup>\*,†</sup> Xiao Cheng Zeng,<sup>\*,¶</sup> and Bing Gong<sup>\*,‡,¶</sup><sup>†</sup>College of Chemistry, Key Laboratory for Radiation Physics and Technology of Ministry of Education, Institute of Nuclear Science and Technology, Sichuan University, Chengdu 610064, Sichuan, China<sup>‡</sup>Department of Chemistry, The State University of New York, Buffalo, New York 14260, United States<sup>#</sup>College of Chemistry, Beijing Normal University, Beijing 100875, China<sup>§</sup>X-ray Operations and Research, Advanced Photon Source, Argonne National Laboratory, 9700 South Cass Avenue, Argonne, Illinois 60439, United States<sup>¶</sup>Department of Chemistry, University of Nebraska—Lincoln, Lincoln, Nebraska 68588, United States<sup>||</sup>National Center for Nanoscience and Technology, Beijing 100190, China

## Supporting Information

**ABSTRACT:** Aromatic oligoamide macrocycles exhibit strong preference for highly directional association. Aggregation happens in both nonpolar and polar solvents but is weakened as solvent polarity increases. The strong, directional assembly is rationalized by the cooperative action of dipole–dipole and  $\pi$ – $\pi$  stacking interactions, leading to long nanotubular assemblies that are confirmed by SEM, TEM, AFM, and XRD. The persistent nanotubular assemblies contain non-collapsible hydrophilic internal pores that mediate highly efficient ion transport observed with these macrocycles and serve as cylindrical sites for accommodating guests such as metal ions.

Many unnatural oligomers that fold into defined shapes are known.<sup>1</sup> We created foldamers with persistent conformations containing lumens from sub-nanometer to >3 nm across.<sup>2</sup> Preparing folding polymers based on the same strategy led to the one-pot formation of macrocycle **1a** in high yields.<sup>3a</sup> This one-pot procedure was then extended to the synthesis of macrocycles such as **2** with much larger sizes,<sup>3b</sup> or those with different backbones.<sup>3c</sup> The availability of cavity-containing, shape-persistent macrocycles<sup>4,5</sup> offers the possibility of creating higher-order structures<sup>6,7</sup> with novel functions.<sup>7d,g</sup> For example, we reported highly conducting transmembrane single-ion channels formed by macrocycles **1** bearing proper side chains.<sup>8</sup> It was proposed that the observed ion transport was mediated by the non-collapsible internal pores of tubular structures formed from aligned macrocycles. Herein we report the strong aggregation of macrocycles **1** and **2**, the nanotubular stacks formed from the directional assembly of these molecules, and the inclusion of metal ions into the internal pores of the nanotubes.

Upon their discovery, macrocycles **1a** were noticed for their strong aggregation. The <sup>1</sup>H NMR spectrum of **1a** recorded in CDCl<sub>3</sub> at room temperature contains no signals, indicating decreased molecular



motion due to aggregation.<sup>9</sup> At 50 °C, the signals of **1a** remain broadened.<sup>3a</sup> The <sup>1</sup>H NMR spectra of **1b** and **1c** recorded in CDCl<sub>3</sub> also show noticeable broadening of signals, especially in the regions of aromatic and amide proton resonances.<sup>10</sup> These early observations prompted us to investigate the intermolecular association of these macrocyclic molecules.

Compounds **1b** and **1c** were examined using <sup>1</sup>H NMR in CDCl<sub>3</sub> by varying concentration and temperature. The <sup>1</sup>H NMR signals of these macrocycles became better resolved at elevated temperatures or decreased concentrations.<sup>10</sup> It was also observed that increasing solvent polarity led to improved resolution of the <sup>1</sup>H NMR signals of **1b** and **1c**.<sup>10</sup>

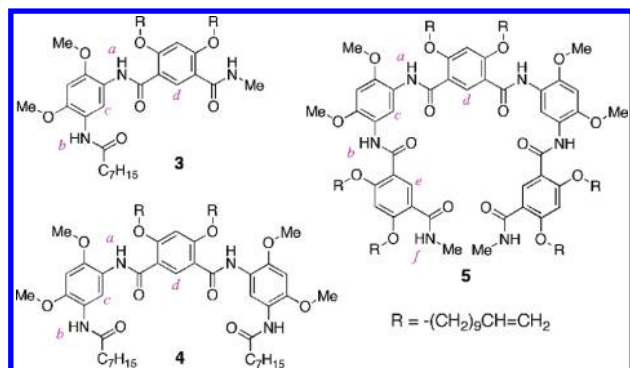
The aggregation of **1b** was confirmed by dynamic light scattering (DLS).<sup>10</sup> In CHCl<sub>3</sub>, the average size of aggregates grew from 550 to 1909 nm as the concentrations of **1b** changed from 0.25 to 5 mM, reached 2045 nm at 9 mM, and leveled off at higher concentrations. Consistent with results from <sup>1</sup>H NMR studies, enhancing solvent polarity decreased the size of the aggregates. In acetone, the average size of the aggregates formed by **1b** (5 mM) was significantly reduced (102 nm) in comparison to that in CHCl<sub>3</sub>. Macrocycle **1c**, being less soluble, showed the same aggregation behavior.<sup>10</sup>

Received: September 10, 2011

Published: October 24, 2011

The above results demonstrate that the aggregation of macrocycles **1a**, **1b**, and **1c** was weakened at elevated temperatures and lowered concentrations and, interestingly, in polar solvents. The intermolecular aggregation initially indicated for **1a** seems to be an inherent property of these macrocycles which share the same oligoamide backbone.

Comparing the  $^1\text{H}$  NMR spectrum of **1b** with those of **3**, **4**, and **5** provided additional details. In  $\text{CDCl}_3$ , Ha of **1b** shows a significant (0.29 ppm) upfield shift compared to Ha of **3**. The amide protons of **4** and **5** also show upfield shifts (0.10 ppm for Ha of **4**; 0.16 ppm for Ha and 0.21 ppm for Hb of **5**) relative to Ha of **3**. Given that the H-bonding capacities of these amide protons are “saturated” upon forming three-center H-bonds,<sup>2c,11</sup> the observed upfield shifts accompanying the larger oligoamides cannot be rationalized by intermolecular H-bonding.



The shifts of the  $^1\text{H}$  NMR resonances of **4** and **5** relative to those of **3**, being proportional to the surface area of the corresponding molecules, reflect the strength of the stacking interaction of these relatively flat molecules.<sup>12</sup> Besides amide protons, the aromatic protons *d* and *c* of **1b** also exhibit pronounced shifts (from 0.3 to 0.4 ppm) relative to the signals of the corresponding aromatic protons of **3**, **4**, and **5**.<sup>10</sup> The large shifts observed for the amide and aromatic protons of **1b** suggest that the cyclic oligoamide backbone has a particularly strong propensity for stacking interaction, which results in especially strong self-aggregation.

The  $^1\text{H}$  NMR spectra of **1b**, **3**, **4**, and **5** recorded in mixtures of  $\text{CDCl}_3$  and  $\text{CD}_3\text{OD}$  revealed that the three-center H-bonded amide protons, although unavailable for additional H-bonding,<sup>2c,11</sup> all exhibited noticeable downfield shifts with increasing  $\text{CD}_3\text{OD}$  content (Figure 1). At 20%  $\text{CD}_3\text{OD}$ , Ha of **4** and Ha and Hb of **5** shifted to positions nearing Ha of **3**, which undergoes the weakest stacking interaction because it has the smallest surface area among these oligoamides.<sup>12</sup> This result suggests that the stacking of **4** and **5** was weakened with increasing solvent polarity. The amide  $^1\text{H}$  signal of **1b**, appearing at much more upfield positions relative to those of **3**, **4**, and **5**, also underwent downfield shifts with increasing solvent polarity, indicating weakened stacking interactions in polar media.  $\text{CDCl}_3$  solvent containing different percentages of other polar solvents including  $\text{DMSO}-d_6$  or  $\text{CD}_3\text{CN}$  also led to the same trend of line-sharpening and downfield shifting, indicating that the observed disruption of aggregation in polar solvents is caused by hydrogen-bonding between solvent molecules and the macrocycles. These observations are consistent with results from earlier  $^1\text{H}$  NMR and DLS studies discussed above.

The effect of solvent polarity on the aggregation of these oligoamides is in contrast to what is known about aromatic

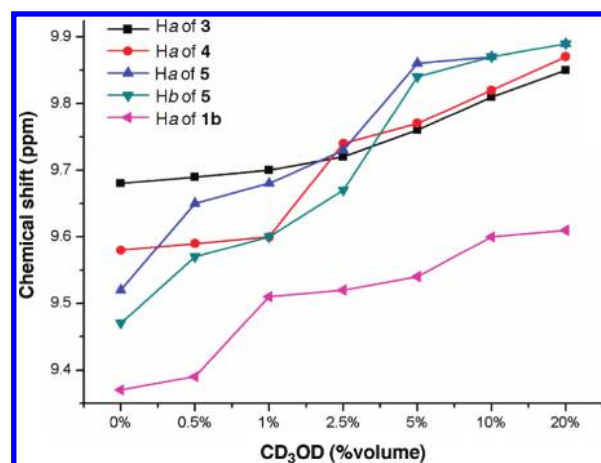


**Figure 1.** Chemical shifts of the three-center H-bonded amide protons of **1b**, **3**, **4**, and **5** (2.0 mM) versus percent of  $\text{CD}_3\text{OD}$  in  $\text{CDCl}_3$ . The  $^1\text{H}$  NMR spectra were recorded at 300 K.

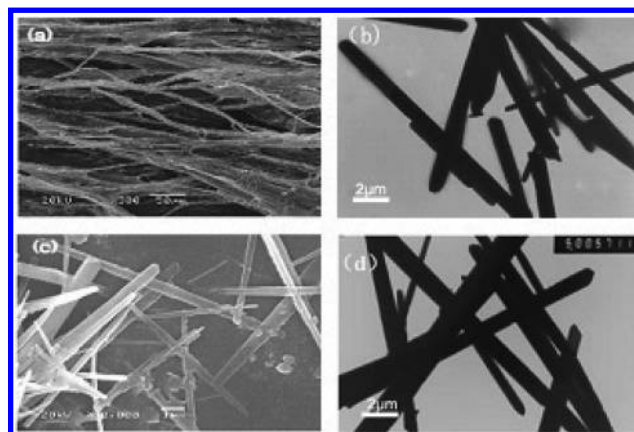


**Figure 2.** (a) SEM (on mica) and (b) TEM (on carbon film) images of the solid samples of **1b**. (c) SEM (on mica) and (d) TEM (on carbon film) images of the solid samples of **2**. All solid samples were formed by drop-casting solutions in  $\text{CHCl}_3$  (for **1b**) or in  $\text{CHCl}_3/p\text{-xylene}$  (2/1, for **2**).

stacking, which is usually promoted in solvents of high dielectric constants, such as water and methanol, and discouraged in solvents of low dielectric constants, such as  $\text{CHCl}_3$ .<sup>13</sup> To explain the observed aggregation and solvent effect, *ab initio* computation was performed. A large binding energy of  $-57.9$  (DFT-D) or  $-55.3$  kcal/mol (DFT-D3) for the association of two molecules of **1d** was revealed.<sup>10</sup> With the shape of a shallow bowl, the macrocycle has a large (15.5D) overall dipole moment passing through the center of the macrocyclic backbone (Figure S82).<sup>10</sup> Being at least 10 times stronger than that of regular  $\pi-\pi$  stacking, the association of these macrocycles is best rationalized by the cooperative action of dipole–dipole and  $\pi-\pi$  interactions.<sup>10</sup> The contribution of a strong dipole–dipole interaction also explains the effect of polar solvents on the aggregation of macrocycles **1**.

The large dipole moment of macrocycles **1** should lead to the alignment or directional assembly of these structurally symmetrical molecules. This expectation was confirmed by examining the assembly of **1b** in the solid state. The scanning electron microscopy (SEM) image of a sample of **1b**, prepared by dropping a solution in  $\text{CHCl}_3$  onto mica followed by evaporating solvent, reveals fibers of over  $400\ \mu\text{m}$  in length and  $2\text{--}3\ \mu\text{m}$  in

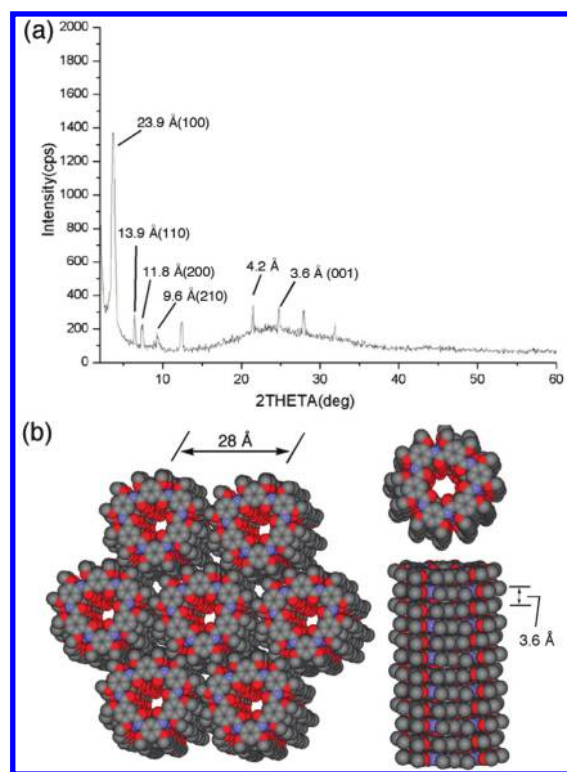


**Figure 3.** (a) Diffractogram of the solid sample of **1b**. (b) Modeling of the columnar packing of **1b** and the hexagonal lattice. The hexagonal lattice parameter  $a$  is 27.6 Å. The orientation of the macrocycles in a column is currently unknown.

diameter (Figure 2a). The transmission electron microscopy (TEM) image of a sample of **1b**, prepared by drop-casting the same solution onto carbon film (Figure 2b) or mesh grid,<sup>10</sup> reveals straight, rod-like assemblies. SEM and TEM of **1c** also reveal similar fibers.<sup>10</sup> Directional assembly is not limited to **1**. SEM and TEM (Figure 2c,d) of **2** show long, rod-like fibers. Additionally, the atomic force microscopy (AFM) images of solid samples of **1b** and **2** reveal long fibers on the surface.<sup>10</sup> These microscopic images point to a highly directional assembly of these largely flat macrocyclic molecules.

Details on the assembly of **1b** were gained from X-ray diffraction (XRD). An intense peak at 23.9 Å and three others at 13.9, 11.8, and 9.6 Å, with ratios of  $d$ -spacings being 1:1/ $\sqrt{3}$ :1/2:1/ $\sqrt{7}$ , are detected (Figure 3a). The XRD pattern points to cylindrical stacks that further packed on a typical hexagonal ( $col_h$ ) lattice (Figure 3b).<sup>14</sup> The lattice parameter  $a$  (27.6 Å), i.e., the intercolumnar spacing, agrees with the diameter of **1b** given partially ( $\sim 55\%$ ) collapsed or interdigitated side chains, which confirms that these molecules aligned into a tubular assembly with its outer and inner diameters being defined by the macrocycles.

Consistent with strong, directional dipole–dipole interaction, the stacked macrocycles exhibit an extraordinary long-range ordering. The 3.60-Å reflection, typical of  $\pi$ – $\pi$  stacking, is attributed to the intra-columnar spacing between the parallel macrocyclic cores, giving a correlation length of 69.6 nm based on Scherrer's equation.<sup>15</sup> This correlation length indicates a nanotube consisting of  $\sim 193$  continuously stacked macrocycles. Similar XRD analysis on the solid samples of **1c** and **2** revealed the same tubular phases in which long columns consisting of large numbers of macrocycles pack on a hexagonal lattice.<sup>10</sup>

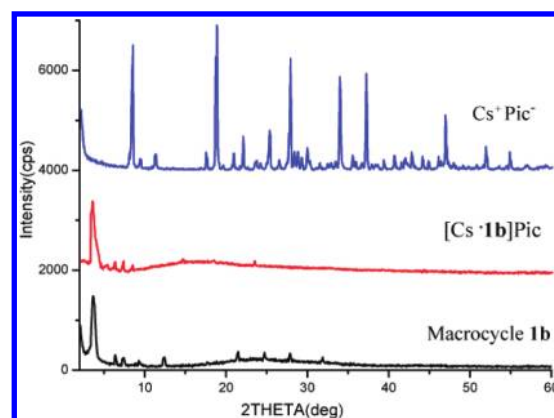


**Figure 4.** Diffractogram of the solid samples of cesium picrate alone, the complex of **1b** with  $Cs^+Pic^-$ , and macrocycle **1b** alone. The stacking distance between adjacent macrocyclic cores is 3.8 Å for the **1b**· $Cs^+Pic^-$  complex.

The confirmed nanotubular assembly of **1b** (and similarly **1c** and **2**) has provided structural evidence confirming the validity of a previously proposed model for explaining the highly conducting ion channels formed by analogues of **1a**–**c**.<sup>8</sup> Besides serving as ion channels, the hydrophilic sub-nanometer pores formed by **1b** should also serve as sites for accommodating polar species, including various metal ions.

This possibility was probed by mixing an excess amount of cesium picrate ( $Cs^+Pic^-$ ) with **1b** in  $CHCl_3$ , in which the salt is nearly insoluble.<sup>10</sup> After filtering off excess  $Cs^+Pic^-$ , the otherwise colorless solution of **1b** became yellow. Removing  $CHCl_3$  left a solid residue with a  $^1H$  NMR spectrum (in  $CDCl_3$ ) containing the signals of **1b** along with that (at 8.78 ppm) of the picrate ion.<sup>10</sup> The presence of  $Cs^+Pic^-$  led to dramatic shifts of the  $^1H$  NMR signals of **1b**. The observed changes suggest complexation of  $Cs^+$  ion by **1b**. By integrating the  $^1H$  NMR signals of the picrate ion and the olefin moiety of the side chains, the stoichiometry of the **1b**· $Cs^+Pic^-$  complex was found to be 1:0.83. DLS measurements revealed that mixing **1b** (2 mM,  $CHCl_3$ ) with  $Cs^+Pic^-$  formed aggregates with an average size of 320 nm. These results indicate that  $Cs^+Pic^-$  underwent strong interaction with the aggregates of **1b**, which suggests that the  $Cs^+$  ions are enclosed within the hydrophilic pores of the nanotubular assemblies. A similar change in the  $^1H$  NMR signals of **1b** was observed upon addition of  $K^+Pic^-$  (Figure S77), suggesting that the hydrophilic pores could accommodate metal ions of different sizes.

In the solid state, directional assembly was observed for **1b** with added  $Cs^+Pic^-$ . SEM of a sample of  $Cs^+Pic^-$  and **1b** (1:1), prepared by drop-casting a  $CHCl_3$  solution onto mica, shows long fibers.<sup>10</sup> XRD of **1b**·( $Cs^+Pic^-$ ) revealed a hexagonal lattice similar to that of **1b** (Figure 4). Lattice parameter  $a$  (28.6 Å), corresponding to the intercolumnar spacing, is very similar to that of pure **1b**. An intra-columnar spacing of 3.8 Å, larger than the 3.6 Å observed for **1b** alone, indicates that the distance between the macrocyclic cores increased in the presence of  $Cs^+$  ions, due likely to electrostatic repulsion. Given the small increase of stacking distance, the picrate ions, instead of being sandwiched between the macrocyclic backbones, are more likely “dissolved” by the alkenyl side chains and located between the columnar stacks. The 3.8-Å reflection gives a correlation length of 77.82 nm,<sup>10</sup> corresponding to a tube consisting of  $\sim 205$



continuously stacked macrocycles. Thus, the columnar assembly and hexagonal packing of **1b** remain in the presence of  $\text{Cs}^+\text{Pic}^-$ , suggesting that the metal ions are complexed within the hydrophilic pore of the nanotubular stacks.

In summary, oligoamide macrocycles undergo strong, directional assembly. In contrast to the stacking of typical aromatic hydrocarbons, aggregation of these macrocycles is weakened in polar media. The interplay of dipole–dipole and  $\pi$ – $\pi$  stacking leads to strong aggregation and the observed effect of solvent polarity. These macrocycles readily form long fibers in the solid state, in contrast to the fabrication of 1D assemblies of many disk-like aromatics, which requires demanding conditions.<sup>16</sup> XRD data reveal well-defined, long nanotubes, which confirms the highly directional stacking of these macrocycles. With their persistent shape, non-deformable cavities, and high propensity of aggregation, tubular assemblies of oligoamide macrocycles provide a reliable supramolecular motif, based on which a variety of organic nanotubes containing non-collapsible internal pores can be created. The ability of **1b** to accommodate metal ions while maintaining the same nanotubular assembling and packing order bodes well for creating new porous materials.

## ■ ASSOCIATED CONTENT

**S Supporting Information.** Experimental procedures, analytical data, and microscopic images. This material is available free of charge via the Internet at <http://pubs.acs.org>.

## ■ AUTHOR INFORMATION

### Corresponding Author

bgong@buffalo.edu; lhyuan@scu.edu.cn; xzeng@unlserve.unl.edu

### Present Address

<sup>†</sup>Key Laboratory of Organo-pharmaceutical Chemistry, Gannan Normal University, Ganzhou 341000, P.R. China

## ■ ACKNOWLEDGMENT

This work is supported by the National Natural Science Foundation of China (20774059, 21172158), the Doctoral Program of the Ministry of Education of China (20090181110047), and the U.S. National Science Foundation (CBET-1036171 and CBET-1066947). Analytical & Testing Center of Sichuan University (Dr. Pengchi Deng) is acknowledged for NMR experiments.

## ■ REFERENCES

- (1) Reviews: (a) Gellman, S. H. *Acc. Chem. Res.* **1998**, *31*, 173. (b) Hill, D. J.; Mio, M. J.; Prince, R. B.; Hughes, T. S.; Moore, J. S. *Chem. Rev.* **2001**, *101*, 3893. (c) Gong, B. *Chem. Eur. J.* **2001**, *7*, 4336. (d) Huc, I. *Eur. J. Org. Chem.* **2004**, *17*. (e) Li, Z. T.; Hou, J. L.; Li, C.; Yi, H. P. *Chem. Asian J.* **2006**, *1*, 766. (f) Goodman, C. M.; Choi, S.; Shandler, S.; DeGrado, W. F. *Nature Chem. Biol.* **2007**, *3*, 252.
- (2) (a) Gong, B. *Acc. Chem. Res.* **2008**, *41*, 1376. (b) Gong, B.; Zeng, H. Q.; Zhu, J.; Yuan, L. H.; Han, Y. H.; Cheng, S. Z.; Furukawa, M.; Parra, R. D.; Kovalevsky, A. Y.; Mills, J. L.; Skrzypczak-Jankun, E.; Martinovic, S.; Smith, R. D.; Zheng, C.; Szyperki, T.; Zeng, X. C. *Proc. Natl. Acad. Sci. U.S.A.* **2002**, *99*, 11583. (c) Yuan, L. H.; Zeng, H. Q.; Yamato, K.; Sanford, A. R.; Feng, W.; Atreya, H. S.; Sukumaran, D. K.; Szyperki, T.; Gong, B. *J. Am. Chem. Soc.* **2004**, *126*, 16528.
- (3) (a) Yuan, L. H.; Feng, W.; Yamato, K.; Sanford, A. R.; Xu, D. G.; Guo, H.; Gong, B. *J. Am. Chem. Soc.* **2004**, *126*, 11120. (b) Feng, W.; Yamato, K.; Yang, L. Q.; Ferguson, J.; Zhong, L. J.; Zou, S. L.; Yuan, L. H.; Zeng, X. C.; Gong, B. *J. Am. Chem. Soc.* **2009**, *131*, 2629. (c)

Ferguson, J. S.; Yamato, K.; Liu, R.; He, L.; Zeng, X. C.; Gong, B. *Angew. Chem., Int. Ed.* **2009**, *48*, 3150.

(4) (a) Bunz, U. H. F.; Rubin, Y.; Tobe, Y. *Chem. Soc. Rev.* **1999**, *28*, 107. (b) Sessler, J. L.; Tvermoes, N. A.; Davis, J.; Anzenbacher, P.; Jursikova, K.; Sato, W.; Seidel, D.; Lynch, V.; Black, C. B.; Try, A.; Andrioletti, B.; Hemmi, G.; Mody, T. D.; Magda, D. J.; Kral, V. *Pure Appl. Chem.* **1999**, *71*, 2009. (c) Grave, C.; Schluter, A. D. *Eur. J. Org. Chem.* **2002**, *2002*, 3075. (d) Zhang, W.; Moore, J. S. *Angew. Chem., Int. Ed.* **2006**, *45*, 4416. (e) MacLachlan, M. J. *Pure Appl. Chem.* **2006**, *78*, 873. (f) Höger, S. *Pure Appl. Chem.* **2010**, *82*, 821.

(5) (a) Yamaguchi, Y.; Yoshida, Z.-I. *Chem. Eur. J.* **2003**, *9*, 5430. (b) Höger, S. *Angew. Chem., Int. Ed.* **2005**, *44*, 3806. (c) Xing, L. Y.; Ziener, U.; Sutherland, T. C.; Cuccia, L. A. *Chem. Commun.* **2005**, 5751. (d) Zhang, W.; Moore, J. S. *J. Am. Chem. Soc.* **2005**, *127*, 11863. (e) Campbell, F.; Wilson, A. J. *Tetrahedron Lett.* **2009**, *50*, 2236. (f) Qin, B.; Ren, C. L.; Ye, R. J.; Sun, C.; Chiad, K.; Chen, X. Y.; Li, Zhao; Xue, F.; Su, H. B.; Chass, G. A.; Zeng, H. Q. *J. Am. Chem. Soc.* **2010**, *132*, 9564. (g) Frischmann, P. D.; Facey, G. A.; Ghi, P. Y.; Gallant, A. J.; Bryce, D. L.; Lelj, F.; MacLachlan, M. J. *J. Am. Chem. Soc.* **2010**, *132*, 3893.

(6) Reviews on columnar/tubular assemblies: (a) Bong, D. T.; Clark, T. D.; Granja, J. R.; Ghadiri, M. R. *Angew. Chem., Int. Ed.* **2001**, *40*, 988. (b) Block, M. A. B.; Kaiser, C.; Khan, A.; Hecht, S. *Top. Curr. Chem.* **2005**, *245*, 89. (c) Keizer, H. M.; Sijbesma, R. P. *Chem. Soc. Rev.* **2005**, *34*, 226. (d) Pasini, D.; Ricci, M. *Curr. Org. Syn.* **2007**, *4*, 59.

(7) Examples of columnar/tubular assemblies: (a) Ghadiri, M. R.; Granja, J. R.; Milligan, R. A.; McRee, D. E.; Khazanovich, N. *Nature* **1993**, *366*, 324. (b) Seebach, D.; Matthews, J. L.; Meden, A.; Wessels, T.; Baerlocher, C.; McCusker, L. B. *Helv. Chim. Acta* **1997**, *80*, 173. (c) Gattuso, G.; Menzer, S.; Nepogodiev, S. A.; Stoddart, J. F.; Williams, D. J. *Angew. Chem., Int. Ed.* **1997**, *36*, 1451. (d) Mindyuk, O. Y.; Stetzer, M. R.; Heiney, P. A.; Nelson, J. C.; Moore, J. S. *Adv. Mater.* **1998**, *10*, 1363. (e) Kim, Y.; Mayer, M. F.; Zimmerman, S. C. *Angew. Chem., Int. Ed.* **2003**, *42*, 1121. (f) Fenniri, H.; Deng, B. L.; Ribbe, A. E.; Hallenga, K.; Jacob, J.; Thiagarajan, P. *Proc. Natl. Acad. Sci. U.S.A.* **2002**, *99*, 6487. (g) Gallant, A. J.; MacLachlan, M. J. *Angew. Chem., Int. Ed.* **2003**, *42*, 5307. (h) Percec, V.; Dulcey, A. E.; Balagurusamy, V. S. K.; Miura, Y.; Smidrkal, J.; Peterca, M.; Nummelin, S.; Edlund, U.; Hudson, S. D.; Heiney, P. A.; Hu, D. A.; Magonov, S. N.; Vinogradov, S. A. *Nature* **2004**, *430*, 764. (i) Pisula, W.; Kastler, M.; Yang, C.; Enkelmann, V.; Mullen, K. *Chem. Asian J.* **2007**, *2*, 51. (j) Yang, J.; Dewal, M. D.; Profeta, S.; Smith, M. D.; Li, Y. Y.; Shimizu, L. S. *J. Am. Chem. Soc.* **2008**, *130*, 612. (k) Fischer, L.; Decossas, M.; Briand, J. P.; Didierjean, C.; Guichard, G. *Angew. Chem., Int. Ed.* **2009**, *48*, 1625. (l) Frischmann, P. D.; Guieu, S.; Tabeshi, R.; MacLachlan, M. J. *J. Am. Chem. Soc.* **2010**, *132*, 7668. (m) Ren, C. L.; Maurizot, V.; Zhao, H. Q.; Shen, J.; Zhou, F.; Ong, W. Q.; Du, Z. Y.; Zhang, K.; Su, H. B.; Zeng, H. Q. *J. Am. Chem. Soc.* **2011**, *133*, 13930. (n) Sato, K.; Itoh, Y.; Aida, T. *J. Am. Chem. Soc.* **2011**, *133*, 13767. (o) Fritzsche, M.; Bohle, A.; Dudenko, D.; Baumeister, U.; Sebastiani, D.; Richardt, G.; Spiess, H. W.; Hansen, M. R.; Hoyer, S. *Angew. Chem., Int. Ed.* **2011**, *50*, 3030.

(8) Helsel, A. J.; Brown, A. L.; Yamato, K.; Feng, W.; Yuan, L. H.; Clements, A.; Harding, S. V.; Szabo, G.; Shao, Z. F.; Gong, B. *J. Am. Chem. Soc.* **2008**, *130*, 15784.

(9) (a) Nelson, J. C.; Saven, J. G.; Moore, J. S.; Wolynes, P. G. *Science* **1997**, *277*, 1793. (b) Brunsveld, L.; Zhang, H.; Glasbeek, M.; Vekemans, J. A. J. M.; Meijer, E. W. *J. Am. Chem. Soc.* **2000**, *122*, 6175.

(10) Please see Supporting Information for details.

(11) Parra, R. D.; Zeng, H. Q.; Zhu, J.; Zheng, C.; Zeng, X. C.; Gong, B. *Chem. Eur. J.* **2001**, *7*, 4352.

(12) Zhang, Y. F.; Yamato, K.; Zhong, K.; Zhu, J.; Deng, J. G.; Gong, B. *Org. Lett.* **2008**, *10*, 4339.

(13) Norberg, J.; Nilsson, L. *Biophys. J.* **1998**, *74*, 394.

(14) Prasad, S. K.; Rao, D. S. S.; Chandrasekhar, S.; Kumar, S. *Mol. Cryst. Liq. Cryst.* **2003**, *396*, 121.

(15) Cullity, B. D.; Stock, S. R. *Elements of X-Ray Diffraction*, 3rd ed.; Prentice-Hall: Englewood Cliffs, NJ, 2001.

(16) Zang, L.; Che, Y. K.; Moore, J. S. *Acc. Chem. Res.* **2008**, *41*, 1596.